FLOW OF A VISCOUS FLUID BETWEEN FIXED AND BLOWN ROTATING DISKS

L. A. Dorfman

NASA TT F-10,931

Translation of "Techeniya vyazkoy zhidkosti mezhdu nepodvizhnym i obduvayemym vrashchayushchimisya diskami."
Izvestiya Akademii Nauk SSSR, Mekhanika Zhidkosti i Gaza,
No. 2, p. 86-91, March-April 1966.

NATIONAL AERONAUTICS AND SPACE ADMINISTRATION
WASHINGTON D.C. 20546 MAY 1967

FLOW OF A VISCOUS FLUID BETWEEN FIXED AND BLOWN ROTATING DISKS

L. A. Dorfman

ABSTRACT. Discussion of the problem of motion of a viscous incompressible fluid in the interspace between an infinite rotating plane and a parallel fixed permeable plane through which supplementary fluid is injected at a constant rate. The problem is solved by solving a system of Navier-Stokes equations.

§ 1. Let us investigate the problem of the motion of a viscous incompressible fluid in the space between an infinite rotating plane and a fixed plane which is parallel to it. An additional fluid passes through this latter plane at a constant rate (Figure 1). /86*

We must solve a system of Navier-Stokes equations in order to calculate the flow in the space between the fixed and rotating planes. These equations are assumed for a steady regime, with allowance for axial symmetry in a cylindrical coordinate system r, ϕ, z having the following form:

$$\begin{aligned} v_r\frac{\partial v_r}{\partial r}+v_z\frac{\partial v_r}{\partial z}-\frac{v_\varphi^2}{r}&=-\frac{1}{\rho}\frac{\partial p}{\partial r}+\nu\left(\frac{\partial^2 v_r}{\partial r^2}+\frac{1}{r}\frac{\partial v_r}{\partial r}-\frac{v_r}{r^2}+\frac{\partial^2 v_r}{\partial z^2}\right)\\ v_r\frac{\partial v_\varphi}{\partial r}+v_z\frac{\partial v_\varphi}{\partial z}+\frac{v_\varphi v_r}{r}&=\nu\left(\frac{\partial^2 v_\varphi}{\partial r^2}+\frac{1}{r}\frac{\partial v_\varphi}{\partial r}-\frac{v_\varphi}{r^2}+\frac{\partial^2 v_\varphi}{\partial z^2}\right)\\ v_r\frac{\partial v_z}{\partial r}+v_z\frac{\partial v_z}{\partial z}&=-\frac{1}{\rho}\frac{\partial p}{\partial z}+\nu\left(\frac{\partial^2 v_z}{\partial r^2}+\frac{1}{r}\frac{\partial v_z}{\partial r}+\frac{\partial^2 v_z}{\partial z^2}\right)\end{aligned} \tag{1.1}$$

Here v_r, v_ϕ, and v_z are the radial, circumferential, and axial velocity components, respectively; p - pressure; ρ - density; ν - kinematic viscosity of the fluid.

The components v_r and v_z are related by the equation of discontinuity

$$\frac{\partial v_r}{\partial r}+\frac{v_r}{r}+\frac{\partial v_z}{\partial z}=0 \tag{1.2}$$

In order to satisfy this equation identically, let us introduce the current function ψ, so that

$$v_z=\frac{1}{r}\frac{\partial\psi}{\partial r},\qquad v_r=-\frac{1}{r}\frac{\partial\psi}{\partial z} \tag{1.3}$$

As may be readily ascertained, the problem under consideration is a self-similar problem.

Actually, if we introduce the functions $f(\zeta)$ and $G(\zeta)$ so that

$$\psi=\omega s r^2 f(\zeta),\quad v_\varphi=r\omega G(\zeta),\quad \zeta=z/s \tag{1.4}$$

where s is the distance between the fixed and rotating walls, then after substituting (1.3), (1.4) in system (1.1) we obtain a system of two ordinary

* Numbers in the margin indicate pagination in the original foreign text.

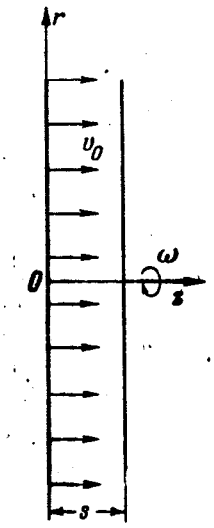

Figure 1

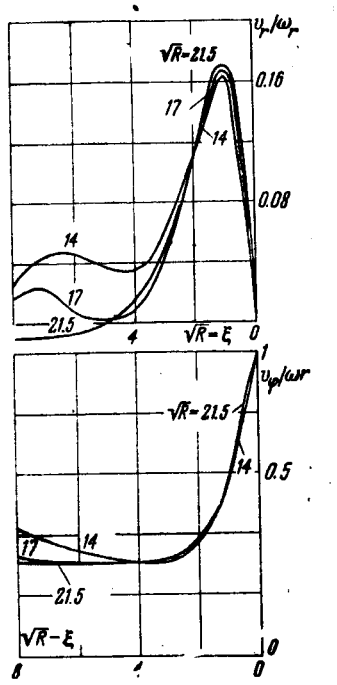

Figure 2

differential equations from the first two equations:

$$\frac{1}{R}f''' - 2ff'' + (f')^2 - G^2 + 2E = 0$$
$$\frac{1}{R}G'' - 2fG' + 2f'G = 0 \qquad (1.5)$$

The third equation yields the following expression for the pressure

$$\frac{p}{\rho} = 2\omega^2 s^2\left(-f^2 + \frac{f'}{R}\right) + Er^2\omega^2 \qquad \left(R = \frac{s^2\omega}{\nu}\right) \qquad (1.6)$$

Here R is the Reynolds number; E - unknown constant. The radial and axial velocity components may be determined by means of $f(\zeta)$ according to the following formulas /87

$$v_r = -\omega r f', \qquad v_z = 2\omega s f \qquad (1.7)$$

The boundary conditions of the problem assume the following form on the fixed wall ($\zeta = 0$)

$$f(0) = \frac{v_0}{2\omega s} = k, \quad f'(0) = 0, \quad G(0) = 0 \qquad (1.8)$$

and the following form on the rotating wall ($\zeta = 1$)

$$f(1) = 0, \quad f'(1) = 0, \quad G(1) = 1 \qquad (1.9)$$

§ 2. The nonlinearity of the numerical solution of the boundary value problem (1.5), (1.8), (1.9) entails some difficulty. In order to solve the problem by the method of trial and interpolation, we must know the values of all the necessary boundary conditions at one of the ends in the first approximation, in order to begin to solve the Cauchy problem. For small R numbers, these approximate solutions may be obtained by expanding the desired quantities in power series

with respect to R.

$$f(\zeta) = f_0(\zeta) + Rf_1(\zeta) + R^2 f_2(\zeta) + \cdots$$
$$G(\zeta) = g_0(\zeta) + Rg_1(\zeta) + R^2 g_2(\zeta) + \cdots \qquad (2.1)$$
$$E = E_0 + RE_1 + R^2 E_2 + \cdots$$

We may satisfy the boundary conditions due to the fact that we set

$$g_0(1) = 1, \qquad f_0(0) = k$$

and otherwise we set f_n, f'_n, g_n equal to zero at both ends.

Substituting (2.1) in (1.5) and setting the coefficients equal to zero for powers of R, with allowance for the boundary conditions for f_n and g_n, we obtain the following expression

$$f_0 = k, \qquad g_0 = \zeta, \qquad E_0 = {}^3/_{20}$$
$$f_1 = {}^1/_{60}\zeta^5 - {}^1/_{20}\zeta^3 + {}^1/_{30}\zeta^2, \quad g_1 = k\zeta(\zeta - 1), \quad E_1 = -{}^7/_{60}k \qquad (2.2)$$
$$f_2 = {}^1/_{360}k(8\zeta^6 - 12\zeta^5 - 9\zeta^4 + 22\zeta^3 - 9\zeta^2)$$
$$g_2 = -{}^1/_{180}({}^4/_7\zeta^7 - {}^9/_5\zeta^5 + \zeta^4 + {}^8/_{35}\zeta) + 2k^2({}^1/_3\zeta^3 - {}^1/_2\zeta^2 + {}^1/_6\zeta)$$

We may use this expression to find the approximate values of the lacking boundary conditions. As the computation shows, particularly for increasing R numbers (and small k) the values of the boundary conditions close to the rotating disk ($\zeta = 1$) will be decisive for solving the nonlinear boundary value problem (1.5), (1.8), (1.9). This corresponds to the physical fact that in this case the rotation of the disk has a decisive influence upon the flow. Therefore, the computation is performed, beginning with the boundary conditions for the case $\zeta = 1$. From formulas (2.2), the first approximations for the lacking boundary conditions have the following form in the case $\zeta = 1$

$$f''(1) = {}^1/_{10}R + {}^2/_{45}kR^2 + \ldots, \quad E = {}^3/_{20} - {}^7/_{60}kR + \ldots$$
$$G'(1) = 1 + kR + ({}^3/_{700} + {}^1/_3 k^2)R^2 + \ldots \qquad (2.3)$$

They were employed to solve the boundary value problem for small R on an ETsVM by the method of trial and interpolation. For increased values of R and k, the values of f'' (1), G' (1) and E were determined in the first approximation according to those found previously by the method of extrapolation, etc.

We should note that with an increase in R there is an increase in the slope representing the derivative of f, G with respect to ζ close to the wall, and the convergence of the successive approximations becomes worse. In order to avoid this, extension of the axis ζ is introduced, so that the new independent variable is not related to the distance s between the walls /88

$$\xi = z\sqrt{\omega/\nu} = \zeta\sqrt{R} \qquad (2.4)$$

and a new function is introduced

$$F = f\sqrt{R} \qquad (2.5)$$

Then, if we designate differentiation with respect to ξ by a dot, we obtain the following system of differential equations from (1.5)

$$F''' - 2FF'' + (F')^2 - G^2 + 2E = 0, \quad G'' - 2FG' + 2F'G = 0 \qquad (2.6)$$

with the boundary conditions

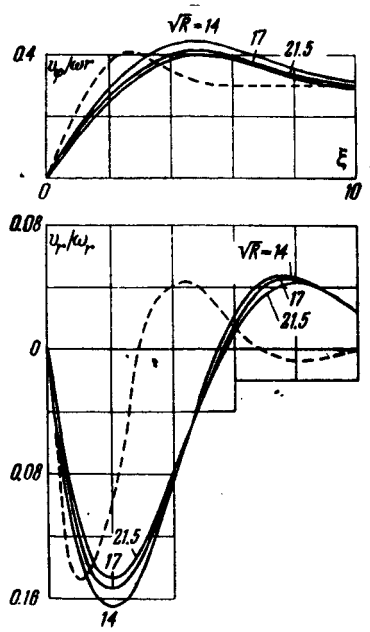

Figure 3

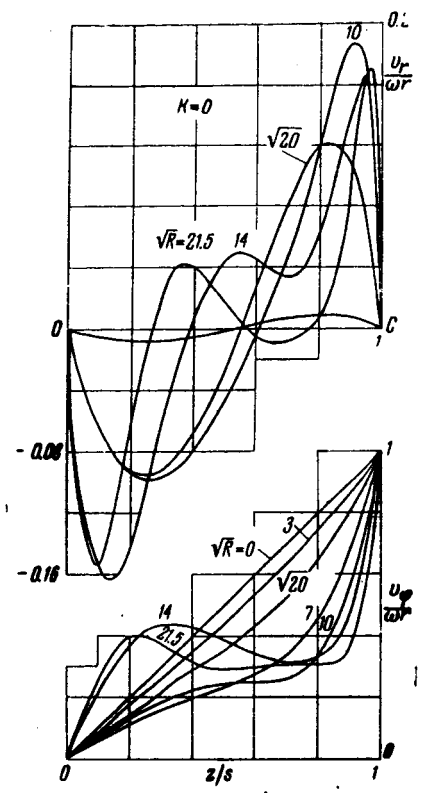

Figure 4

$$G(0)=0,\quad G(\sqrt{R})=1,\quad F(\sqrt{R})=F'(\sqrt{R})=F'(0)=0$$
$$F(0)=k\sqrt{R} \tag{2.7}$$

We thus have

$$f'(\zeta)=F(\xi),\quad G'(\zeta)=G'(\xi)\sqrt{R},\quad f''(\zeta)=F''(\xi)\sqrt{R}$$
$$\tau_r=\mu\frac{\partial v_r}{\partial z}\frac{\mu r\omega}{s}f''(\zeta)=\rho r\nu^{1/2}\omega^{3/2}F''(\xi),\quad \tau_\varphi=\mu\frac{\partial v_\varphi}{\partial z}=\frac{\mu r\omega}{s}G'(\zeta)=\rho r\nu^{1/2}\omega^{3/2}G'(\xi) \tag{2.8}$$

The introduction of the variable ξ for a large dimensionless distance $\sqrt{R}$ between the planes is suggested by experience in solving the corresponding problems for a disk rotating in infinite space [see, for example (Ref. 1)]. A numerical solution of the differential equations (2.6) was performed on an ETsVM by the Runge-Kutta method with automatic selection of the step [modification of Merson (Ref. 2)] within an accuracy of 10^{-7}. The programming was done by J. Z. Serazetdinov.

§ 3. Let us present the computational results. Let us first investigate /89 the case in which there is no blowing (k = 0). We should point out that Grohne (Ref. 3) studied this case; however, he performed computations only to $\sqrt{R}$ = 10. Attention should be called (Table 1) to the monotonic change, as a function of $\sqrt{R}$, of the basic flow parameters characterizing the pressure E and the friction components at the walls (F'' (0), F'' ($\sqrt{R}$), G' (0), G' ($\sqrt{R}$)). Stabilization of these quantities sets in only after $\sqrt{R}$ = 20, just like the velocity component distributions (Figures 2, 3). We may assume that, when the dimensionless

distance s $\sqrt{\omega}/\nu = \sqrt{R}$ increases between the walls, the flow close to the rotating wall must approximate the case investigated by Rogers and Lance (Ref. 1), when the flow rotates at a certain angular rate $\omega' < \omega$ far from the plane rotating at the angular rate ω.

TABLE 1

Case k = 0

$\sqrt{R}$	$F''(0)$	$F''(\sqrt{R})$	$G'(0)$	$G'(\sqrt{R})$	E
1	0.0665	0.1000	0.9987	1.0043	0.1496
3	0.1710	0.2932	0.3051	0.4343	0.1250
4	0.1777	0.3729	0.2006	0.4427	0.0939
$\sqrt{20}$	0.1704	0.4003	0.1664	0.4592	0.0788
5	0.1579	0.4305	0.1337	0.4793	0.0637
6	0.1304	0.4671	0.0986	0.5133	0.0420
7	0.1064	0.4887	0.0769	0.5376	0.0288
9	0.0819	0.5078	0.0631	0.5616	0.0188
10	0.0865	0.5096	0.0695	0.5636	0.0204
12	0.1661	0.4760	0.1363	0.5311	0.0495
14	0.1867	0.4605	0.1533	0.5148	0.0578
15	0.1826	0.4620	0.1500	0.5150	0.0561
17	0.1699	0.4684	0.1440	0.5198	0.0513
20	0.1607	0.4747	0.1319	0.5258	0.0473
21	0.1615	0.4748	0.1324	0.5259	0.0475
21.5	0.1618	0.4747	0.1327	0.5259	0.0476

At the same time, the case of Bödewadt (Ref. 4) occurs close to the fixed wall, when the flow rotates at the angular rate ω'' above the fixed base. Utilizing both of these solutions, we find that $\omega_0 \approx 0.31$ and $E = \omega_0^2/2 \approx 0.048$ from the condition $\omega' = \omega'' = \omega_0$. We thus obtain $F''(\sqrt{R}) \approx 0.474$, $G'(\sqrt{R}) \approx 0.53$ for the rotating wall. The computational results strive to these values when $\sqrt{R}$ increases, as may be seen from the velocity distribution. However, for the fixed wall we obtain essentially different results: instead of $F''(0) \approx 0.291$, $G'(0) \approx 0.24$, according to Bödewadt, we obtain $F''(0) = 0.1618$, $G'(0) = 0.1327$ here. This difference is illustrated by the velocity distribution close to the fixed wall (Figure 3) -- the curves do not approach the Bödewadt curves (shown by the dashed line) when $\sqrt{R}$ increases.

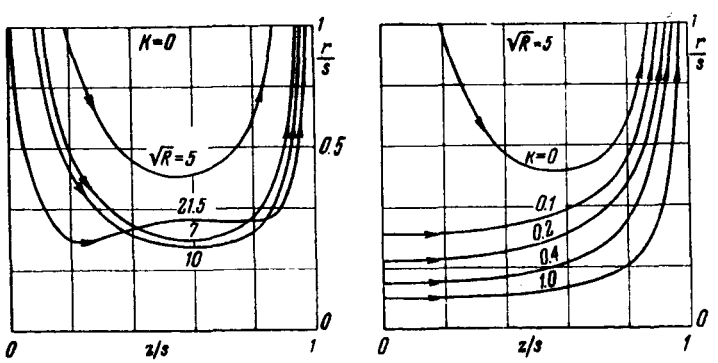

Figure 5

The result obtained may be explained by the fact that for a rotating plane the boundary layer begins to develop from the axis of rotation and is propagated

up to infinity. Therefore, the flow close to the rotating wall approximates the case of the rotation of a disk in a rotating flow as one recedes from the fixed wall. A boundary layer on the fixed plane begins to be formed at in- /90
finity. Therefore, if a rotating wall, and not a rotating flow, is located at infinity -- as in the case of Bödewadt -- a completely different result must be obtained. This is apparent in the fact that, if in the case of large $\sqrt{R}$ there is a section whose circumferential velocity component is almost constant, then this is not true for the radial component, and we cannot speak of two boundary layers at the walls separated by a core rotating like a rigid body (Figure 4).

TABLE 2

k	$\sqrt{R}=1$	3	5	10
		$F''(0)$		
0	0.0665	0.1710	0.1579	0.0865
0.1	—0.5259	—0.0737	—0.0329	—0.0196
0.2	—1.0940	—0.2333	—0.1075	—0.0453
0.4	—2.1620	—0.4436	—0.2020	—0.0903
0.6	—3.1468	—0.6076	—0.3004	—0.1336
0.8	—4.0571	—0.7613	—0.3868	—0.1754
1.0	—4.9015	—0.9119	—0.4759	—0.2172
		$F''(\sqrt{R})$		
0	0.1000	0.2932	0.4305	0.5096
0.1	0.7076	0.5052	0.5343	0.5503
0.2	1.3300	0.7560	0.7173	0.7081
0.4	2.6203	1.4029	1.2996	1.2561
0.6	3.9720	2.2303	2.0886	2.0183
0.8	5.3865	3.2101	3.0352	2.9405
1.0	6.8644	4.3202	4.1136	3.9958
		$G'(0)$		
0	0.9987	0.3051	0.1337	0.0695
0.1	0.8948	0.1153	0.0091	0
0.2	0.8018	0.0431	0.0005	0
0.4	0.6439	0.0056	0	0
0.6	0.5171	0.0007	0	0
0.8	0.4152	0.0001	0	0
1.0	0.3332	0	0	0
		$G'(\sqrt{R})$		
0	1.0043	0.4343	0.4793	0.5636
0.1	1.0921	0.6286	0.6435	0.6683
0.2	1.1762	0.7807	0.7772	0.7833
0.4	1.3344	1.0248	1.0134	1.0101
0.6	1.4813	1.2255	1.2134	1.2081
0.8	1.6184	1.3998	1.3879	1.3820
1.0	1.7472	1.5556	1.5441	1.5378
		E		
0	0.1496	0.1250	0.0637	0.0204
0.1	—0.4769	—0.0107	—0.0147	—0.0196
0.2	—1.1338	—0.1544	—0.1076	—0.0906
0.4	—2.5428	—0.5412	—0.4123	—0.3613
0.6	—4.0839	—1.0959	—0.9010	—0.7992
0.8	—5.7633	—1.8275	—1.5551	—1.4030
1.0	—7.5869	—2.7357	—2.3795	—2.1720

We should point out that the nature of the velocity distribution and its change with an increase in R corresponds in qualitative terms with the measurements of Daily and Nece (Ref. 5). Their velocity profiles have characteristic

bends corresponding to the calculations (see the curves for $\sqrt{R} = 14$ and $\sqrt{R} = 21.5$ in Figure 4). With an increase in R, there is a section having a constant circumferential component. However, a quantitative agreement cannot be expected, in view of the fact that the experiments were performed with disks limited by a cylindrical housing and with a turbulent flow regime, in addition.

/91

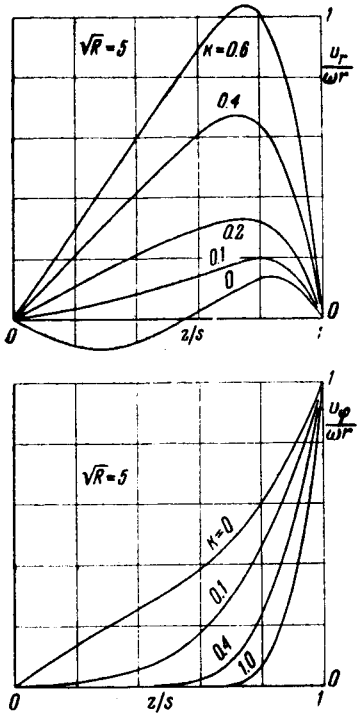

Figure 6

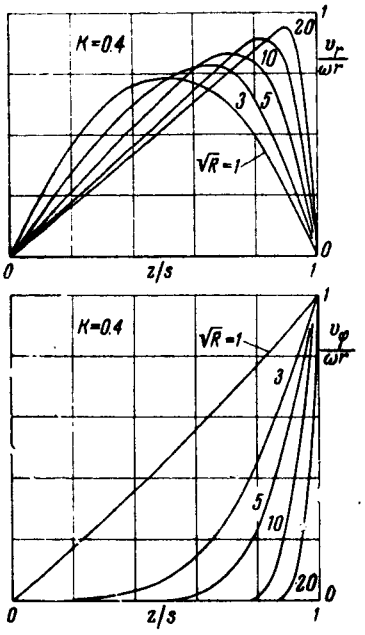

Figure 7

The nature of the change in the current surfaces with an increase in R is of interest. Taking the dimensionless function of the current in the following form

$$\psi^{\circ} = \frac{\psi}{\omega s^3} = \left(\frac{r}{s}\right)^2 \frac{F}{\sqrt{R}}$$

we may characterize the current surface for a given R by compiling a graph of $\psi^{\circ} = 1$, i.e.,

$$\frac{r}{s} = \left(\frac{\sqrt{R}}{F}\right)^{1/2}$$

With an increase in R, the current lines press closer to the walls (Figure 5), and there is a characteristic bend in the current surfaces.

We should point out that an insignificant blast ($k \leq 0.1$ in the case $\sqrt{R} < 20$) suppresses the inflow in the direction of the medium axis of rotation along the fixed wall (Figures 5 and 6), and a convex profile of the radial velocities develops. The flow twist is extinguished close to the fixed wall. For a given blast (k = const), the twist is also extinguished with an increase in the R number close to the fixed wall. The flow input with the rotating wall is increased, and the maximum of the radial velocity profile approaches that of the rotating wall (Figure 7). Correspondingly, when there is a fixed distance between the walls the

components of friction stress on the rotating wall increase, and they decrease on the fixed wall. The influence of the blast intensity k and the Reynolds number R upon the friction stress components at the walls and upon the pressure is shown in Table 2. In particular, it is apparent that with an increase in R the blast intensity k must increase when the medium inflow is suppressed along the fixed wall (i.e., in order that F" (0) = 0).

REFERENCES

1. Rogers, M.H., Lance, G.N. The Rotationally Symmetric Flow of a Viscous Fluid in the Presence of an Infinite Rotating Disk. J. Fluid Mech., Vol. 7, No. 4, 1960.
2. Lance, G.N. Numerical Methods for Computers. Izdatel'stvo Innostrannoy Literatury, 1962.
3. Grohne, D. The Laminar Flow in a Circular, Cylindrical Box. Nachrichten Acad. Wiss. Göttingen. Math -- Phys. Kl., No. 1, 1956.
4. Bödewadt, U.T. Rotational Flow over a Rigid Base. Z. angew. Math. und Mech., V. 20, No. 5, p. 241-253, 1940.
5. Daily, J.W., Nece, R.E. Chamber Dimension Effects of Enclosed Rotating Disks, J. Basic Engng., Trans. ASME, Ser. D, Vol. 82, No. 1, 217-232, 1960.

Scientific Translation Service
4849 Tocaloma Lane
La Canada, California
NASw 1496